LAWRENCE
LIVERMORE
NATIONAL
LABORATORY

LLNL-PROC-425265

Photoacoustically Measured Speeds of Sound and the Equation of State of HBO2: On Understanding Detonation with Boron Fuel

J. M. Zaug, S. Bastea, J. Crowhurst, M. Armstrong, L. Fried, N. Teslich

March 9, 2010

14th International Detonation Symposium
Coeur d'alene, ID, United States
April 11, 2010 through April 16, 2010

Disclaimer

Photoacoustically Measured Speeds of Sound and the Equation of State of HBO_2: On Understanding Detonation with Boron Fuel

Joseph M. Zaug, Sorin Bastea, Jonathan C. Crowhurst, Michael R. Armstrong, Laurence E. Fried, and Nick E. Teslich Jr.

Lawrence Livermore National Laboratory
Physical and Life Sciences, PO BOX 808, L-350, Livermore CA 94551

Abstract. Elucidation of geodynamic, geochemical, and shock induced processes is limited by challenges to accurately determine molecular fluid equations of state (EOS). High pressure liquid state reactions of carbon species underlie physiochemical mechanisms such as differentiation of planetary interiors, deep carbon sequestration, propellant deflagration, and shock chemistry. In this proceedings paper we introduce a versatile photoacoustic technique developed to measure accurate and precise speeds of sound (SoS) of high pressure molecular fluids and fluid mixtures. SoS of an intermediate boron oxide, HBO_2 are measured up to 0.5 GPa along the 277 ˚C isotherm. A polarized exponential-6 interatomic potential form, parameterized using our SoS data, enables EOS determinations and corresponding semi-empirical evaluations of >2000 ˚C thermodynamic states including energy release from bororganic formulations. Our thermochemical model propitiously predicts boronated hydrocarbon shock Hugoniot results.

Introduction

Earth's evolving geochemistry involves complex reactions between silicate solutions, mantle minerals, oxides, and other molecules with high pressure hydrocarbon species. Physical conditions predominate in the upper- and lower-mantle, including those generated by explosive volcanism, can be created by ignition of rocket propellants, or during explosive crystallization or detonation processes. The addition of metal reactants to enhance the performance of these tools increases their chemical similarities with interior planetary processes. Metal additives were first introduced to energetic material formulations to increase the impact potential of shaped charges.[1] Predictions of reaction products from highly energetic CHNO materials containing metal additives are a highly empirical and limited primarily to large-scale calibration tests and knowledge of sparsely available extreme condition thermodynamic data. Aluminum powder was observed to decrease shock pressure and reaction velocities of HEs, an effect attributed to low heat of formation oxide products at the Chapman-Jouguet, (C-J) plane of explosives, i.e. the thermodynamic state where the products behind a steady propagating detonation front reach chemical equilibrium.[2] Boron was also recognized as a candidate additive allowing for its high volumetric heat of reaction, 137.45 kJ/cc, which is the highest elemental ΔH per unit volume.[3] An early

detonation rate study indicated that ammonium nitrate mixed with 10wt%, boron (particle size of 10 μm) will form B_2O_3 at approximate pressures and temperatures of 2.5-20 GPa and 2273-4273 ˚C.[4] When 5-10wt% of a secondary HE, PETN, was added to this mixture, the overall detonation velocity increased 25% for the largest charge diameter. The notion was that PETN increased the reaction temperature from 1973 ˚C to 4773 ˚C, which enabled complete oxidation of boron thus liberating additional thermochemical energy. Guidance leading to this supposition was based upon the pioneering work of Macek and Semple where boron (particle sizes 34.5 and 44.2 μm) was reported to undergo a two-stage oxidation sequence; ignition followed by combustion.[5] Initially a B_2O_3 passivating layer forms via gas phase reactions with available oxidizer(s). If the detonation temperature exceeds the high pressure melt temperature of B_2O_3, combustion of the underlying pure boron occurs. Akimov et al. reported the effect of boron (particle size of 0.1 μm) on the detonation velocity of three HEs exhibiting a wide range of oxygen balance. Upon increasing the boron content from 4.5wt% to 11wt% they measured a loss of 3.5% in the detonation velocity of PETN.[6] Under the same HE:boron mixture range reported by Akimov et al., Pepekin et al. determined nearly identical heats of explosion for PETN and RDX.[7] More recently Sezaki et al. observed a 20% increase in detonation velocity of a formulated polymer blended explosive (PBX=73wt% RDX and 27wt% hydroxyl terminated polybutadiene binder) when boron (particle size ≤44 μm) content was increased from 4wt% to 10wt%.[8]

The significance of the boron particle size on combustion dynamics was highlighted by a study reported by Yeh and Kou: 3 μm diameter particles more quickly reach the ambient pressure melting temperature of 2723 ˚C resulting in virtually no "dark region" between the ignition and combustion stages.[9] The correlation between burning time and particle diameter was recently extended to nano-scale lengths by Young et al.[10] They found a weak dependence on the ignition and combustion stage oxidation rates with particle diameter. The available mole fraction of oxygen primarily altered the combustion rate while particle temperature strongly affected the rates of each reaction stage. Interestingly they found that for nano-scale boron there is a temperature threshold required to achieve complete combustion. This phenomenon is attributed to convective and radiative heat loss; submicron particles are unable to generate sufficient heat to melt pure boron. The energy source for second-stage combustion of $(BO)_n$ species, formed when pure boron dissolves into molten B_2O_3, is attributed to highly exothermic reactions with H_2O vapor and molecular oxygen. To summarize, the reaction sequence of boron according to Yeh and Kou follows,

Ignition:
$4/3B(s)+4/3B_2O_3(l)+2H_2O(g)+O_2(g) \rightarrow 4\ HBO_2(g)$

Combustion:
$2B(l)+ O_2(g) \rightarrow B_2O_2\ (g)$

Intermediate reaction steps form additional boroxides. However, when H_2O is present, HBO_2 is shown to be the most thermodynamically stable product between 1873 – 2673 ˚C in oxygen-rich environments.[11] As Yetter et al. demonstrated in their combustion kinetics study, and Young and Sullivan et al. later reiterate, oxidizer-rich and wet environments enable HBO_2 to lock or trap boron thus preventing complete oxidation.[10 - 12] To circumvent the poisoning effect H_2O has on boron oxidation, Ulas et al. explored suggestions made by several researchers that fluorine-containing environments may enhance the removal of $B_2O_3(l)$ and, by fluoro-reduction of HBO_2, increase global energy release.[13] The fluorination of boron results in a 79% increase in volumetric ΔH compared to ΔH of oxidation.[3] Their results demonstrate that for 1μm and 3μm particle size boron the total burning time decreases only after the fluorine to oxygen (Fl/O) ratio exceeds 0.47, a point where free fluorine begins to replace less reactive HF molecular product. The Fl/O ratio must exceed approximately 2.2 before total burning time falls below that of Fl/O = 0. The previously mentioned two-stage combustion reaction reduces to one continuous burn sequence when Fl/O exceeds 0.07 and the B_2O_3 surface temperature exceeds 2293 ˚C; HF and especially atomic fluorine vaporize the $B_2O_3(l)$ layer much more rapidly than H_2O and

O_2.[13] Oxidizers react with pure boron at faster rates than HF, and at much slower rates than F. Shock-tube reaction studies (8.5 atm.) reported by Spalding et al. (3-5μm particle size) indicate that boron oxidation rates drop significantly when adding N_2 in dry environments.[14] Macek and Semple demonstrated that N_2 will accelerate boron oxidation when H_2O is available.[5]

A stringently tested semi-empirical thermochemical model would quantify the conditions that poison oxidation reactions and suggest reactant stoichiometries to unlock the fuel potential of metal additives. Ulas et al. provided a simplified semi-empirical oxidation and fluorination model for boron combustion; however, it is strictly limited to near ambient pressure conditions. We hypothesize that boron containing CHNO HEs will produce HBO_2, which to a significant degree affects energy output, just as it does in combustion reactions.[15] There are no experimental or theoretical data available to construct a semi-empirical HBO_2 equation of state, so we chose to measure elevated pressure SoS. The SoS is the most sensitive state variable to changes in a materials EOS. Variations to compressed fluid speeds of sound typically exceed measurement error by factors of 10^3. Direct volume measurements of compressed fluids cannot approach such high fidelity in precision.

Experimental Approach

In these proceedings we discuss a novel in situ technique developed to measure SoS of virtually any translucent fluid encapsulated in a chamber by transparent windows. The heated diamond-anvil cell (DAC) is utilized to control sample pressure and temperature. SoS data enable parameterization of interatomic potential functions, from which extreme condition thermodynamic states are calculated. Normally we employ the impulsive stimulated light scattering (ISLS) technique to launch and probe ultrasonic waves within fluid samples.[16-17] The technical advantages of ISLS to study fluids have been previously discussed.[18] However there are practical requirements for optically thin, e.g., <50 μm DAC sample fluids, 1) they must absorb minimally 0.1% of excitation pulse light and, 2) exhibit no photo reactions with either excitation or probe pulses. Unfortunately HBO_2(l) does not absorb at the fundamental or higher harmonics of our 1064 nm excitation source. Furthermore we observe a high propensity for initiation of HBO_2(s) photochemistry by two overlapped ISLS excitation pulses (1.0-1.4 GW/cm^2 peak Gaussian profile irradiance). These issues were overcome by developing an experimental approach utilizing one attenuated excitation pulse (<0.4GW/cm^2 peak Gaussian profile irradiance) to launch pressure waves into translucent fluids or solids.

To generate coherent broadband sound waves, first a platinum film is deposited onto the culet of a diamond-anvil. Focused ion beam (FIB) site specific deposition is conducted using a FEI Nova600i NanoLab instrument. A culet is first cleaned and then coated with 150-200 Å of carbon to minimize FIB charging effects. A precursor gas, trimethyl platinum (TMP) is introduced approximately 200 μm above a culet surface. TMP interacts with a scanning ion beam whereby Pt deposition occurs at the culet surface. We initially found that four parallel Pt films, (0.5-1.0 μm wide, approximately 75 μm long, and 0.27-μm tall), with center-to-center line separations of 22, 25, 30, and 33 μm enables one to measure speeds of sound with velocities ranging from 0.5 to at least 5 km/sec (Figs. 1 and 2). The more simple method of welding micron dimensional wire onto one anvil by method of compression with an opposing anvil may also work to form a transducer

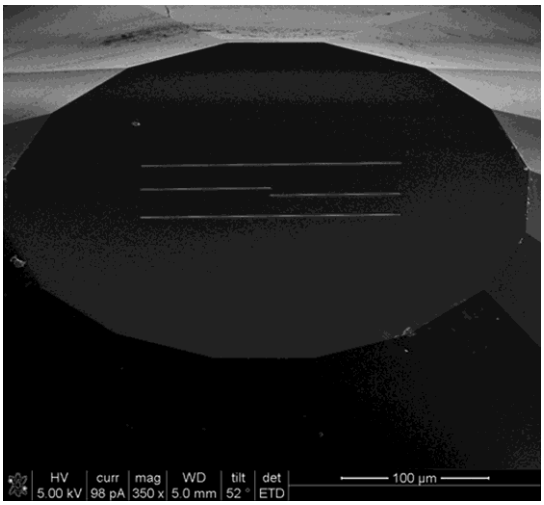

Fig. 1. A SEM image of platinum films deposited onto a diamond-anvil.

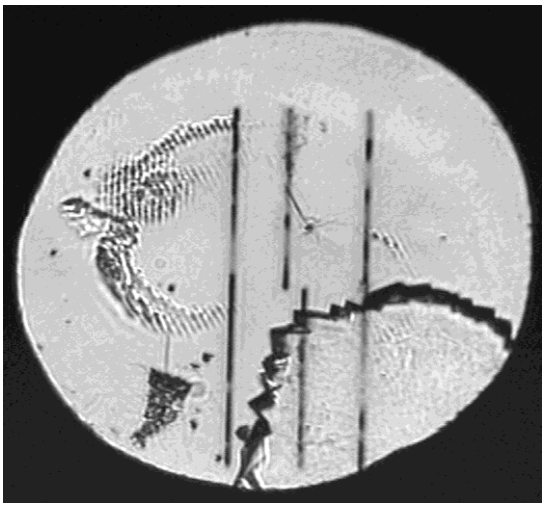

Fig. 2. A photo-micrograph of a DAC sample chamber. At 0.22 GPa and 277 ˚C solid HBO_2 begins to slowly encroach on the remaining supercooled fluid. Inspection of the left side of the chamber reveals gratings that were burned into the culet from failed attempts to generate traditional ISLS signals. A pressure manometer rests in the lower left region of the chamber.

To generate sound, a 100 ps width optical pulse is focused onto a platinum film. The peak laser irradiance on the film, <0.03 GW/cm^2, impulsively increases temperature within the film (electron-phonon energy transfer) by a few degrees. The temperature rise produces a thermal stress distribution in the Pt film that launches a longitudinal strain-pulse. The pulse energy is reflected and transmitted at the interface between the film and the surrounding sample. Transmitted broadband pulses that travel perpendicular to the direction of the excitation-pulse and into the surrounding medium are utilized to make SoS measurements. The physics behind similar photoacoustic transducers is well documented however the geometry and application of our device is unique.[19 – 22] At 277 ˚C and 0.01GPa, the impedance of Pt ≈ 8.8.0x10^7 Kg/s·m^2 and HBO_2(l) = 6.5x10^5 Kg/s·m^2 and so the transmitted acoustic intensity, I_T = 2.9% of that initially within the film; this value increases with applied pressure because the fluid is more compressible, e.g., $I_T \approx$ 4.2% at 0.5 GPa. The leading pulse peak (expansion of the medium) increases and the pulse trench (rarefaction following expansion of the medium) reduces the nominal index of refraction of the sample and therefore alters the local magnitude of optical diffraction. A time-of-flight delayed 532 nm probe-pulse (~ 20 μm FWHM spot) is focused onto a second and parallel Pt film. The probe-pulse peak irradiance is insufficient to photoacoustically launch a pressure wave. (In principle a continuous-wave laser probe and a sufficiently fast GHz range detector and oscilloscope could be employed to expedite data acquisition.) The probe radiation scatters off of the Pt films forming a local oscillator (LO) or reference field, E_R, (I_R=E_R^2) with a constant phase. Probe radiation also diffracts from the traveling wave, generating a diffracted field, E_D (I_D=E_D^2) with a time-varying phase. The LO central frequency is unshifted whereas the diffracted field components are Stokes or anti-Stokes shifted thus leading to the notion of heterodyne detection.[23] A pin-hole aperture is positioned behind the DAC to select a signal collection wave-vector, K_S and pass a narrow cone of light (<1x10^{-4} % of the available DAC solid angle) to a photomultiplier tube, (PMT). Signal intensity measured at the PMT is equal to the square of the mixed fields, and is modulated by the time varying optical phase difference between E_R and E_D. The frequency of the material response is given by $\nu_A = 2c/\lambda_P \ (\sin\theta/2)$, where c is the medium SoS, λ_P is the probe wavelength, and $\theta = \theta_{Pi} + \theta_{Pd}$, the probe angle of incidence and the probe angle of diffraction. The phenomenon described here is analogous to Thomas Young's well known double-slit diffraction experiment where here the slit separation, i.e. the distance between a traveling wave and the point where I_R is generated, is time dependant.[24] Time-domain series (Fig. 3) are Fourier transformed to compute modulation frequency (ν_A < 2 GHz for θ = 10˚, c ≤ 6 km/sec, λ_P = 532 nm). For the sake of brevity we give this technique the abbreviation, PALS (Photoacoustic Light Scattering).

The value of K_S is determined by conducting PALS measurements on a material with accurately established speeds of sound, e.g. speeds of sound collected from water and ice at a measured temperature and determined pressure. PALS

measurements compare favorably with the well-established IAPWS-95 formulations (standard

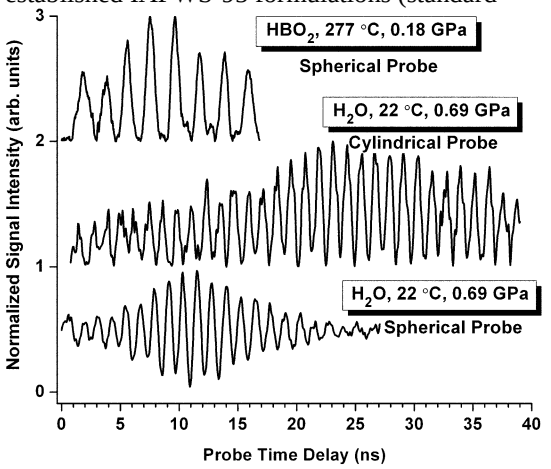

Fig. 3. Normalized PALS time-domain data, offset to enhance clarity, from liquid H_2O and HBO_2.

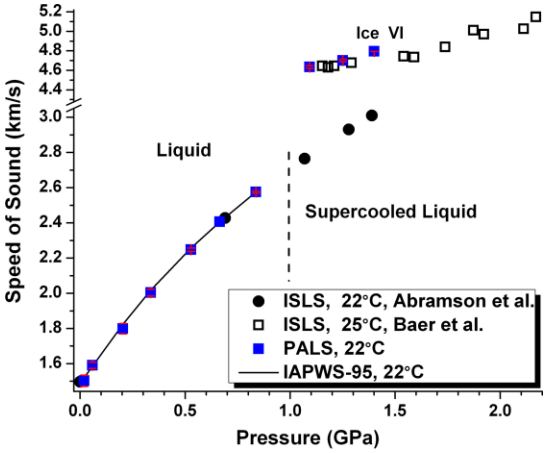

Fig. 4. Determination of K_S is accomplished by measuring ν_A from a sample of known c(P,T). K_S was selected using the IAPWS-95 value for H_2O SoS at 0.66 GPa (blue square with no error bars) and 22 ˚C; PALS data compare well with liquid and solid state measurements by Abramson and Baer.[17,26]

deviation is 0.6%) including accurate ISLS results (Fig. 4).[17,25,26] A powerful feature of PALS allows for a continuum of K_S values to be rapidly changed to investigate dispersion relations without need to physically change θ_{Pi} or the sample position (ν_A = 0.4 – 4.0 GHz for θ = 5˚ - 53˚, c = 2.4 km/sec, and λ_P = 0.532 μm). High P-T adiabatic SoS are determined by, $c = \nu_A / K_S$. Recent improvements, e.g., the use of a cylindrical probe profile, have reduced the error to <0.5%..

Sample Preparation and Characterization

99 % pure HBO_2 (Aldrich), consisting of a powdered mixture of orthorhombic and monoclinic allotropes, was loaded into DAC sample chambers where Ir gaskets were used for radial confinement. The physical properties of HBO_2 have been reported over a wide temperature and pressure range.[27-31] Strontium tetraboride, (STB) doped with approximately 2% Sm served as a pressure manometer with 0.02 GPa precision. The pressure calibration and also temperature corrections specific to our STB are given respectively by Datchi et al. and Abramson et al.[32,17] Separate μ-FTIR measurements were conducted on HBO_2 up to 0.7 GPa along the 277 ˚C isotherm and back to ambient conditions, including post SoS measurement IR data, confirmed molecular stability. At 277 ˚C HBO_2 begins to slowly freeze above 0.22 GPa. In this pressure range the interpolated melting curve is relatively steep, 490 ˚C/GPa. Above 300-350 ˚C, the STB manometer consistently failed within 60 minutes; perhaps the oxidation potential of the fluid increased. The narrow P-T region where fluid-state HBO_2 measurements are accessible may explain the lack of any previous data. Above 300 ˚C a cubic boron nitride optical Raman manometer was required, which has an approximate precision of 0.3 GPa. At 550 ˚C and 2.6 GPa, 10-20 micron diameter vesicles form. Increasing temperature to 650 ˚C at 0.7 – 1.7 GPa caused vesicles to combine and form into a more opaque material comprised of 1-10 micron particles. Corresponding Raman data (<200 kW/cm^2 average Gaussian profile irradiance) reveals the existence of B-O stretch (801 cm^{-1}) and two O-H stretch vibrations (3590 cm^{-1}, and 3623 cm^{-1}).

Discussion

The SoS data obtained from fluid HBO_2 (Fig. 5) provide an opportunity for deriving effective molecular interactions for the HBO_2 molecule,

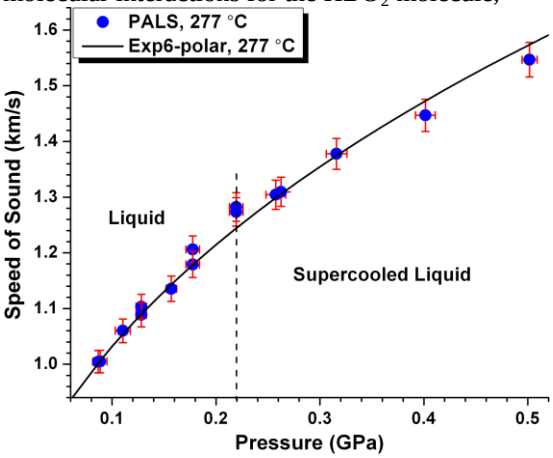

Fig. 5. Measured SoS from HBO_2(l), filled circles, and calculated SoS from Exp6-polar function, solid line.

thus enabling predictions of thermodynamic and chemical equilibrium states of high temperature deflagration, explosive crystallization, or detonation of boron containing compounds. To this end we employ an exp6-polar thermodynamics theory that was previously shown to yield very good results for the properties of hot, dense H_2O and HNO_2.[33,34] HBO_2 is also a strongly polar molecule, with a dipole moment greater than H_2O; for the purpose of the present modeling we set the value of its dipole moment to the calculated value for the isolated molecule, μ = 2.78 Debye.[35] It is possible and quite likely that, similarly with H_2O, a somewhat larger value of μ may be more appropriate for describing HBO_2 at the high-density fluid conditions typical of detonation or high pressure combustion, whose properties we eventually wish to predict. However, the limited experimental data presently available do not warrant trying to discern such an effect; we expect that this approximation will have little effect on our conclusions regarding the character of detonations containing boron, which at this point can only be largely qualitative. We find that exp6 parameter values, r_o = 3.976, ε = 216.3, and α = 12.67 using the above dipole moment yield good agreement with the sound speed measurements - see Fig. 5. Thermodynamic calculations using these parameters place the critical point of HBO_2 approximately at T_c = 447 ˚C and P_c = 260 atm; of course chemical reactivity may actually intervene before these conditions can be reached.

The important role that molecular HBO_2 is likely to play in hydrocarbon or organometallic explosive combustion of boron particles e. g. rocket propellants, is well documented.[3,5,11-15] Here we attempt to quantify its impact in the detonation of explosives containing elemental boron by employing newly determined HBO_2 thermodynamics in the calculation of detonation velocities. These calculations are performed using the code CHEETAH and are similar with those described for example in ref. 36. The code is used here to determine C-J points of explosives. Detonation product results are constrained to single-phase fluid mixtures and, potentially, many condensed phases. The major boron-containing products likely to be relevant for such processes have been discussed for example in ref. 11. The fluid phase components we consider are small molecular products such as N_2, CO_2, H_2O, CO, NH_3, CH_4, HBO_2, O_2, H_2, etc., which are thermodynamically favored at high temperatures and pressures; they are all modeled by exp6 or exp6-polar interactions and tested favorably against experimental data. The condensed phases are carbon (diamond and graphite), B_2O_3 (liquid and solid), B (solid and liquid), BN (solid cubic and hexagonal), CB_4 (solid) and H_3BO_3 (solid), all described by Murnaghan-type EOS. Among these B_2O_3 is of particular importance; it is likely the oxidation end-point of boron. Unfortunately B_2O_3 experimental data are quite scarce. We note that our liquid EOS is in good agreement with the simulation results of Ohmura et al., and the melting line agrees well with that reported by Brazhkin et al..[37-39] Nevertheless, such uncertainties i.e., lack of EOS data from other likely products, likely limit one's confidence to make fully quantitative predictions.

The combustion of solid boron particles is plagued by well known kinetics issues, which are probably important in the detonation of explosives loaded with metallic boron, just as in the case of aluminum-loaded compositions.[10] We attempt to circumvent these complications and focus therefore on explosive mixtures with boronated

organic compounds, which were studied experimentally.[6] Examples are: 1) 86% (by weight) pentaerythritol tetranitrate ($C_5H_8N_4O_{12}$) + 14% orthocarborane ($C_2B_{10}H_{12}$), 2) 75% tetranitromethane (CN_4O_8) + 25% pentaborane (B_5H_9), and 3) 70% tetranitromethane + 30% borazine ($B_3N_3H_6$); their initial densities are ρ_o = 0.78, 1.14, and 1.28 g/cc, respectively. The experimental detonation velocities reported in ref. 6 are D_{exp}=4.64, 5.9, and 6.3 km/s; our corresponding calculated values are, respectively, D_{calc} = 4.78 (Δ=3.02%), 5.96 (Δ=1.02%) and 6.13 (Δ=-2.70%) km/s, indicating reasonable agreement. For these energetic mixtures we discover that the major detonation products containing boron are HBO_2 and B_2O_3(l) (mixture-2 also yields a small amount of liquid boron), mixed with the molecular detonation products typical for CHNO explosives. We show for example in Fig. 6 the C-J point composition of mixture-3, which indicates, as expected, that large amounts of water also result upon detonation.

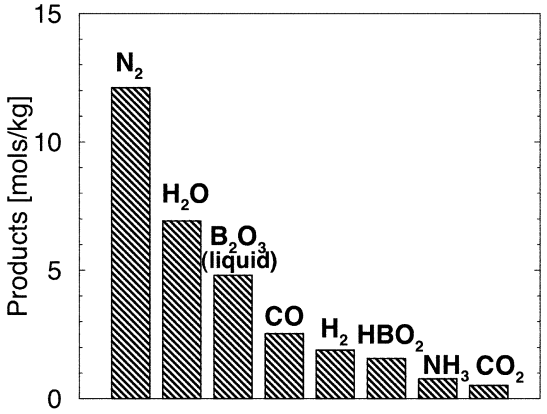

Fig. 6. Calculated C-J plane decomposition mixture from 70% tetranitromethane + 30% borazine ($B_3N_3H_6$).

Summary

Since the reaction of B_2O_3 (l) + H_2O(v) is likely an important route toward the formation of HBO_2, its study at high temperatures and pressures will ultimately advance quantitative predictions of the thermodynamic and kinetic behavior of boron containing explosives and propellants. However the collection of accurate SoS data through currently available in situ measurement techniques is hindered by materials high photosensitivity and/or small P-T regions of chemical stability. We have attempted to overcome these challenges through development of a low-irradiance photoacoustical light scattering technique. SoS data collected on HBO_2(l), suggests, albeit somewhat prematurely, that we can begin to develop EOS based thermochemical models to semi-empirically study/predict deflagration and detonation chemistry involving boron. For example our results for the melting curve of B_2O_3 compare well with recent experimental data and this relatively stringent and successful confirmation adds a new level of confidence for computing metal assisted detonation products and concentrations. Given the relative simplicity and low expense required to perform PALS type measurements, it is our expectation that the example presented here will assist research initiatives directed to understand a wide-array of extreme condition chemical processes.

Acknowledgements

J. M. Z. is grateful to J. M. Brown, and E. H. Abramson for stimulating and thoughtful discussions. This research was funded by the DOE Campaign-II and Joint DoD/DOE Munitions Technology Programs and performed under the auspices of the U.S. Department of Energy by Lawrence Livermore National Laboratory under contract DE-AC52-07NA27344. The authors thank Kimberly Budil (now a senior advisor to the Under Secretary for Science at the U. S. DOE) and Bruce Watkins, LLNL program managers, for their continued support of our research.

References

1. Cook, M. A., Filler, A. S., Keyes, R. T., Partridge, W. S., and Ursenbach, W. O., "Aluminized explosives" *J. Chem. Phys*., Vol. 61, pp 189-196, 1957.

2. Fickett W.; Davis, W. C., "Detonation Theory and Experiment" Dover Publications: Mineola New York, 1979

3. Peretz, A., "Some theoretical considerations of metal-fluorocarbon compositions for ramjet fuels" *Proceedings of the Eighth International Symposium on Air Breathing Engines*, pp. 398-403, Cincinnati, OH, June 14-19, 1987.

4. Sosnova, G. S., "Combustion of boron and aluminum to their higher oxides at high pressures and temperatures" *Materials of the third All-Union Symposium on Combustion and Explosion*, pp 455-458, Leningrad, 1971.

5. Macek, A., and Semple, J. M., "Combustion of boron particles at atmospheric conditions" *Combustion Science and Technology*, Vol. 1, pp 181-191, 1969.

6. Akimov, L. N., Apin, A. Ya., and Stesik, L. N., "Detonation of explosives containing boron and its organic derivatives" *Combustion Explosion and Shock Waves*, Vol. 8, pp 387-390, 1972.

7. Pepekin, V. I., Makhov, M. N., and Apin, A. Ya., "The reactions of boron in the presence of an explosion" *Combustion Explosion and Shock Waves*, Vol. 8, pp 109-111, 1972.

8. Sezaki, T., Date, S., and Satoh, J.-i. "Study on the effects of addition of boron particles to RDX-based PBX regarding prevention of Neumann effect" *Mats. Sci. Forum*., Vols. 465-466, pp 195-200, 2004.

9. Yeh, C. L., and Kuo, K. K., "Ignition and combustion of boron particles" *Energy Combust. Sci.*,Vol. 22, pp 511-541, 1997.

10. Young, G., Sullivan, K., Zachariah, M. R., and Yu, K., "Combustion characteristics of boron nanoparticles" *Combustion and Flame*, Vol. 156, pp 322-333, 2009.

11. Yetter, R. A., Rabitz, F. L., Dryer, F. L., Brown, R. C., and Kolb, C. E.,"Kinetics of high-temperature B/O/H/C chemistry" *Combustion and Flame*, Vol. 83, pp 43-62, 1991.

12. Sullivan, K., Young., G., and Zachariah, M. R., "Enhanced reactivity of nano-B/Al/CuO MIC's" *Combustion and Flame*, Vol., 156, pp 302-309, 2009.

13. Ulas, A., Kuo, K., and Gotzmer, G., "Ignition and combustion of boron particles in fluorine-containing environments" *Combustion and Flame*, Vol., 127, pp 1935-1957, 2001.

14. Spalding, M. J., Krier, H., and Burton, R. L., "Boron suboxides measured during ignition and combustion of boron in shocked Ar/F/O2 and Ar/N2/O2 mixtures" *Combustion and Flame*, Vol., 120, pp 200-210, 2000

15. Meschi, D. J., Chupka, W. A., and Berkowitz, J., "Heterogeneous reactions studied by mass spectrometry. I. Reactions of B_2O_3(s) with H_2O(g)" *J. Chem. Phys.*, Vol. 33, pp 530-533, 1960.

16. Zaug, J. M., Slutsky, L. J., and Brown, J. M., "Equilibrium properties and structural relaxation in methanol to 30.4 GPa" *J. Phys. Chem. B*., Vol. 98, pp 6008-6016, 1994.

17. Abramson, E. H., and Brown, J. M., "Equation of state of water based on speeds of sound measured in the diamond-anvil cell" *Geochimica Et Cosmochimica Acta*, Vol. 68, pp 1827-1835, 2004.

18. Yan, Y.-X., and Nelson, K. A., "Impulsive stimulated light scattering. II. Comparison to frequency-domain light-scattering spectroscopy*" J. Chem. Phys.*, Vol. 87, pp 6257-6265, 1987.

19. Tas, G., and Maris, H. J., "Electron diffusion in metals studied by picosecond ultrasonics" *Phys. Rev. B*, Vol. 49, pp 15046-15054 (1994).

20. Pezeril, T., Ruello, P., Gougeon, S., Chigarev, N., Mounier, J. M., Picart, P., and Gusev, V., "Generation and detection of plane coherent shear picoseconds acoustic pulses y lasers: Experiment and theory" *Phys. Rev. B*., Vol. 75, pp 174307-1-19, 2007.

21. Kou, C.-Y., Vieira, M. M. F., Patel, C. K. N., "Transient optoacoustic pulse generation and detection" *J. Appl. Phys*., Vol. 55, pp 3333-3336, 1984.

22. "Physical Acoustics" ed. Mason, W. P., and Thurston, R. N., Vol. XVIII, Academic Press, INC., 1988.

23. Crimmons, T. F., Stoyanov, N. S., and Nelson, K. A., "Heterodyned impulsive stimulated Raman scattering of phonon-polaritons in $LiTaO_3$ and

$LiNbO_3$" *J. Chem. Phys*., Vol. 117, pp 2882-2896, 2002.

24. Young, T. "The Bakerian lecture: Experiments and calculations relative to physical optics" *Proc. Royal Soc. London A*, Vol. 94, pp 1-16, 1804.

25. "Release of the IAPWS Formulations 1995 for the Thermodynamic Properties of Ordinary Water Substances for General and Scientific Use," International Association for the Properties of Water and Steam, 1996.

26. Baer, B. J., Brown J. M., Zaug, J. M., Schiferl, D., and Chronister, E. L., "Impulsive stimulated scattering in ice VI and ice VII" *J. Chem. Phys*., Vol. 108, pp 4540-4544, 1997.

27.F. C. Kracek, G. W. Morey, and H. E. Merwin, *Amer. J. Sci.*, 35A, 143, (1938).

28. P. Broadhead, and G. A. Newman, *J. Molec. Struc*. 10, 157, (1971).

29. Gilson, T. R., "Characterization of ortho- and meta-boric acids in the vapour phase" *J. Chem. Soc. Dalton Trans*., Iss. 9, pp 2463-2466, 1991.

30. Andrews, L., and Burkholder, T. R., "Infrared spectra of molecular B(OH)3 and HOBO in solid argon" *J. Chem. Phys*., Vol. 97, pp 7203-7210, 1992.

31. Pereira, A. S., Perottoni, C. A., and da Jornada, J. A. H., "Raman spectroscopy as a probe for in situ studies of pressure-induced amorphization: some illustrative examples" *J. Raman Spect.*, Vol. 34, pp 578-586, 2003.

32. Datchi, F., LeToullec, R., and Loubeyre, P., "Improved calibration of the SrB_4O_7:Sm^{2+} optical pressure gauge: Advantages at very high pressures and temperatures" *J. Appl. Phys*., Vol. 81, pp 3333-3339, 1997.

33. Bastea, S., and Fried, L. E., "Exp6-polar thermodynamics of dense supercricital water" *J. Chem. Phys*., Vol. 128, 17502, 2008.

34. Maiti, A., Bastea, S., Howard, W. M., and Fried, L. E., "Nitrous acid under high temperature and pressure – From atomistic simulations to equations of state for thermochemical modeling" *Chem. Phys. Lett*., Vol. 468, pp 197-200, 2009.

35. Dewar, M. J. S., JIE, C. X., and Zoebisch, E. G., "AM1 calculations for compounds containing boron" *Organometallics*, Vol. 7, pp 513-521, 1988.

36. Scott, H. P., Hemley, R. J., Mao, H. K., Herschbach, D. R., Fried, L. E., Howard, W. M., and Bastea, S., "Generation of methane in the Earth's mantle: In situ high pressure-temperature measurements of carbonate reduction" *Proc. Nat. Acad. Sci.*, Vol. 101, pp 14023-14026, 2004.

37. Ohmura, S., and Shimojo, F., "Anomalous pressure dependence of self-diffusion in liquid B2O3: An ab initio molecular dynamics study" *Phys. Rev. B*, Vol. 80, pp 020202(R), 2009.

38. Brazhkin, V. V., Katayama, Y., Inamura, Y., Kondrin, M. V., Lyapin, A. G., Popova, S. V., and Voloshin, R. N., "Structural Transformations in liquid, crystalline, and glassy B2O3 under high pressure" *J. E. T. P. Lett*., Vol. 78, pp 393-397, 2003.

39. Brazhkin, V. V., Katayama, Y., Inamura, Y., Kondrin, M. V., Lyapin, A. G., Popova, S. V., and Voloshin, R. N., "Structural Transformations in liquid, crystalline, and glassy B2O3 under high pressure [JETP Lett. 78 (6), 393-397 (2003)]" *J. E. T. P. Lett*., Vol. 79, p 308, 2004